

# Cosmology with Planck-detected clusters: A new multi-wavelength analysis

*Gaspard Aymerich*

*Marian Douspis, Laura Salvati*

Institut d'Astrophysique Spatiale

*Gabriel Pratt*

Astrophysique Interactions Multi-Echelles, CEA

*Felipe Andrade-Santos, William Forman, Christine Jones*

Center for Astrophysics, Harvard

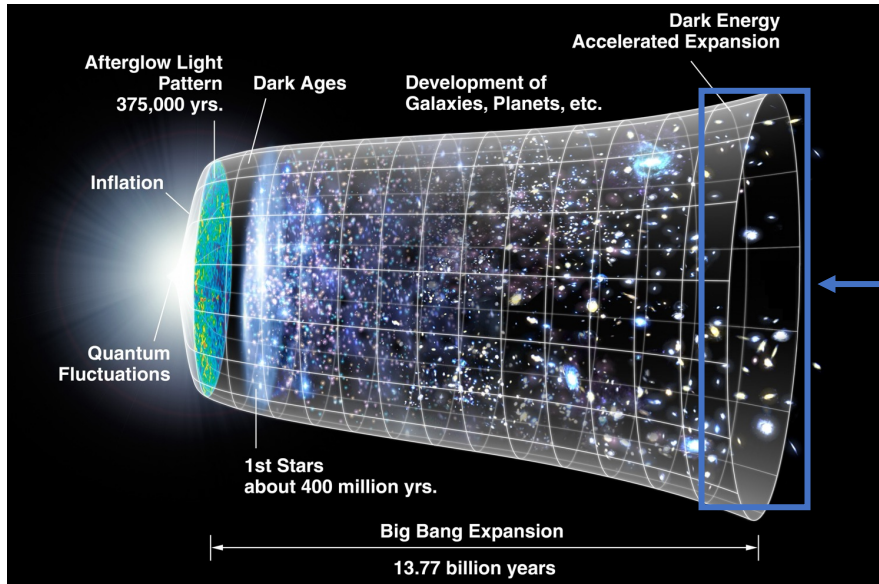
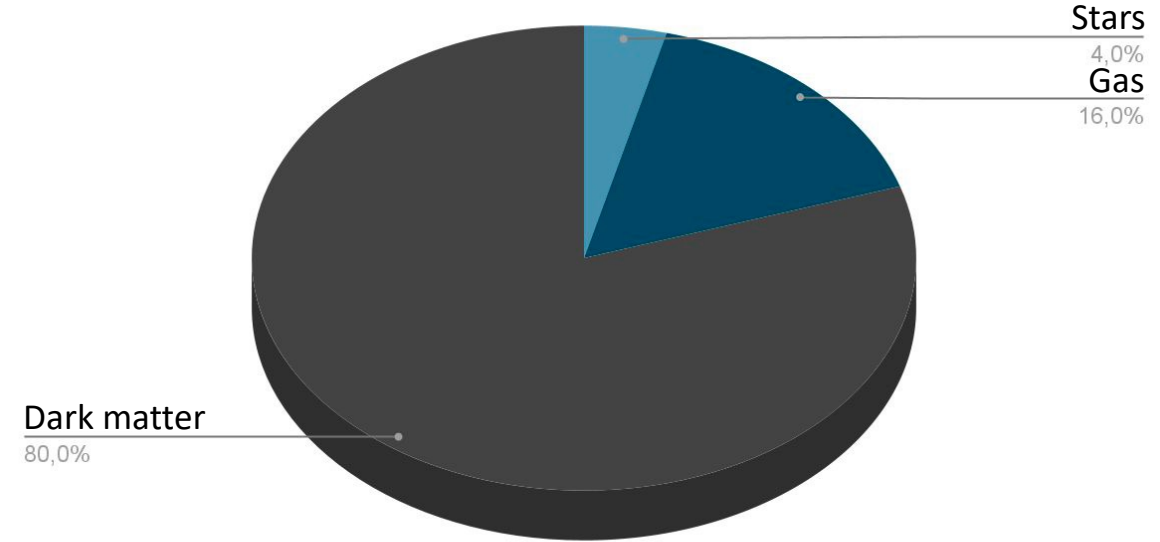
# Cosmology with Galaxy Clusters: an improved multi-wavelength analysis

## Galaxy clusters:

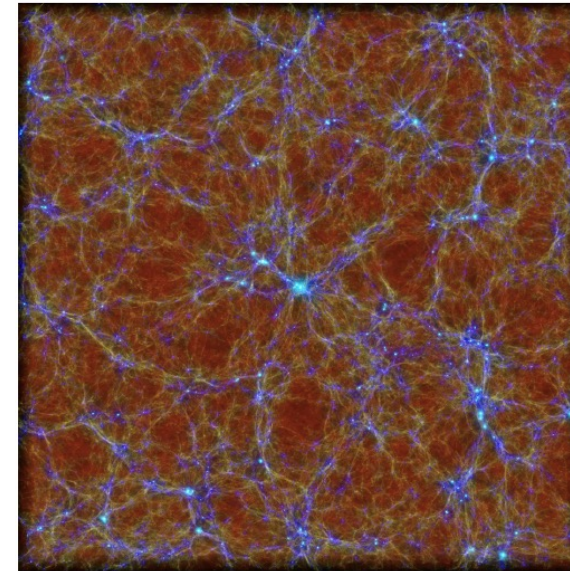
Largest gravitationally bound structures in the Universe, peaks in the cosmic web

Formation at late times

Complex systems with galaxies but also hot gas and dark matter



Hubble Space Telescope Science Institute

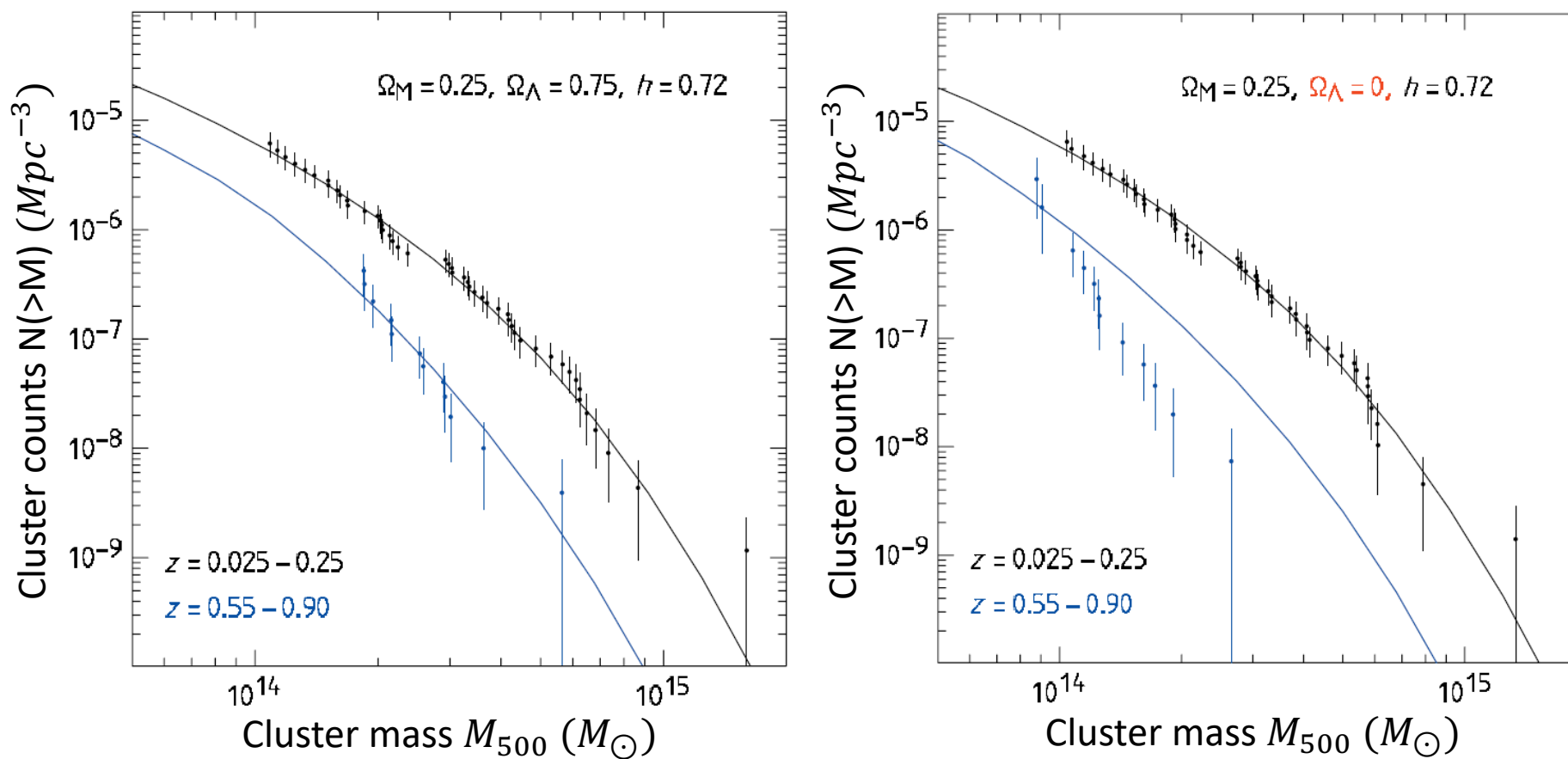


Hirschmann et al. 2014

# Cosmology with Galaxy Clusters: an improved multi-wavelength analysis

How can galaxy clusters be used as a cosmological probe ?

Mass function: theoretical prediction of cluster abundance as function of mass and redshift



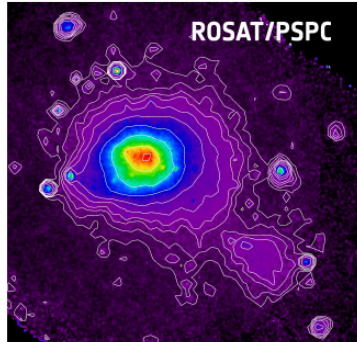
Vikhlinin et al. 2009

# Observing galaxy clusters

How can we observe them ?

Different wavelengths probe different properties of clusters

Combining all wavelengths allow for more precise characterisation of cluster properties



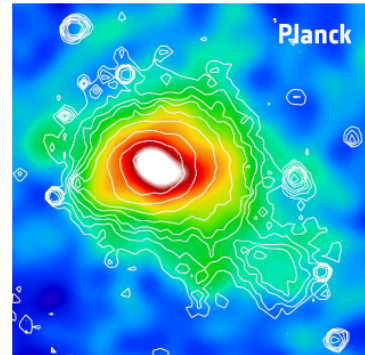
X-ray emission:

**Bremmstrahlung**

Sensitive to **gas density squared**

High resolution

$$E_X \propto \int_V n_e^2 \Lambda(T) dV$$



mm-wavelength:

**Thermal Sunyaev-Zeldovich effect**

(inverse Compton scattering)

Sensitive to **gas pressure**

$$F_\nu \propto \int_\Omega (P = n_e T) d\Omega$$



Optical/near IR wavelength:

**Stars** (small part of total mass)

**Gravitational lensing**

(total mass, limited precision)

# Combining X-ray and SZ

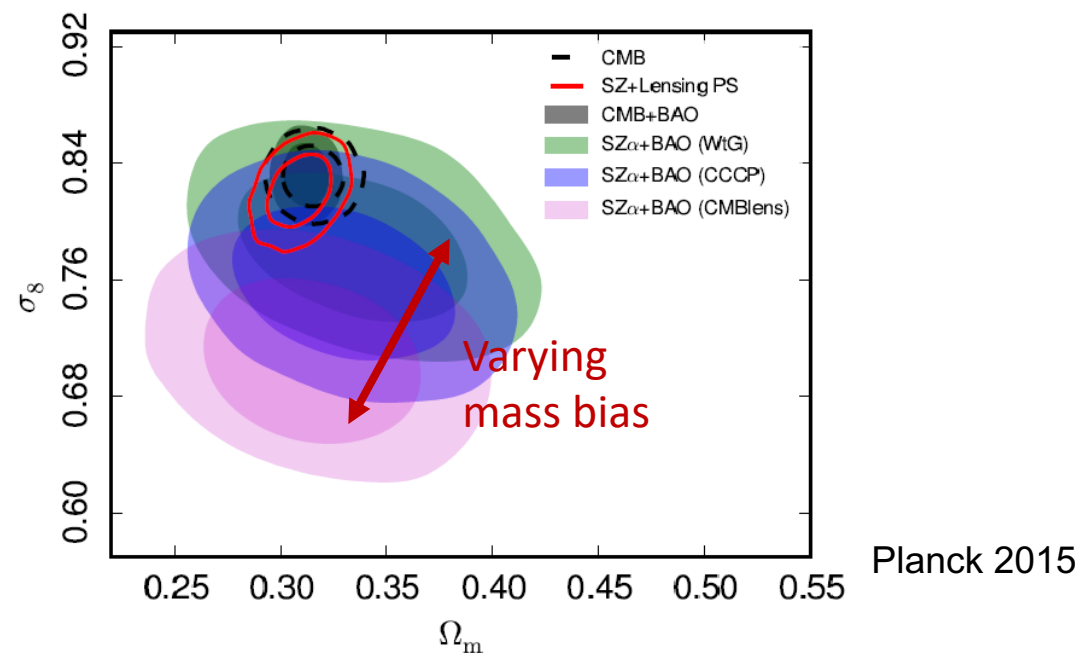
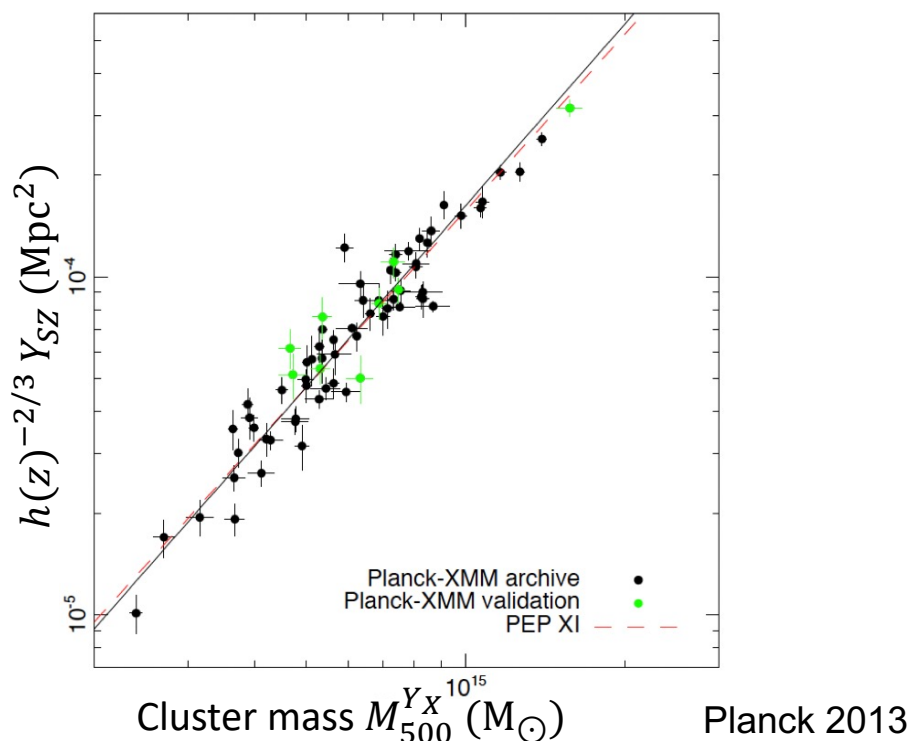
## Improving on Planck 2015: a better calibration sample

Planck data provides full sky SZ-survey: great opportunity for cosmological analysis

Cluster mass can't be directly inferred from SZ signal

Arnaud et al. 2010 relates X-ray signal from XMM-Newton to mass under hydrostatic equilibrium assumption

Y500-M500 is calibrated on a common XMM/SZ set of 71 clusters:  $E^{-2/3}(z) \left[ \frac{D_A^2 Y_{500}}{10^{-4} \text{ Mpc}^2} \right] = 10^{-0.19 \pm 0.02} \left( \frac{(1-b) M_{500}}{6 \times 10^{14} M_\odot} \right)^{1.79 \pm 0.08}$



# Combining X-ray and SZ

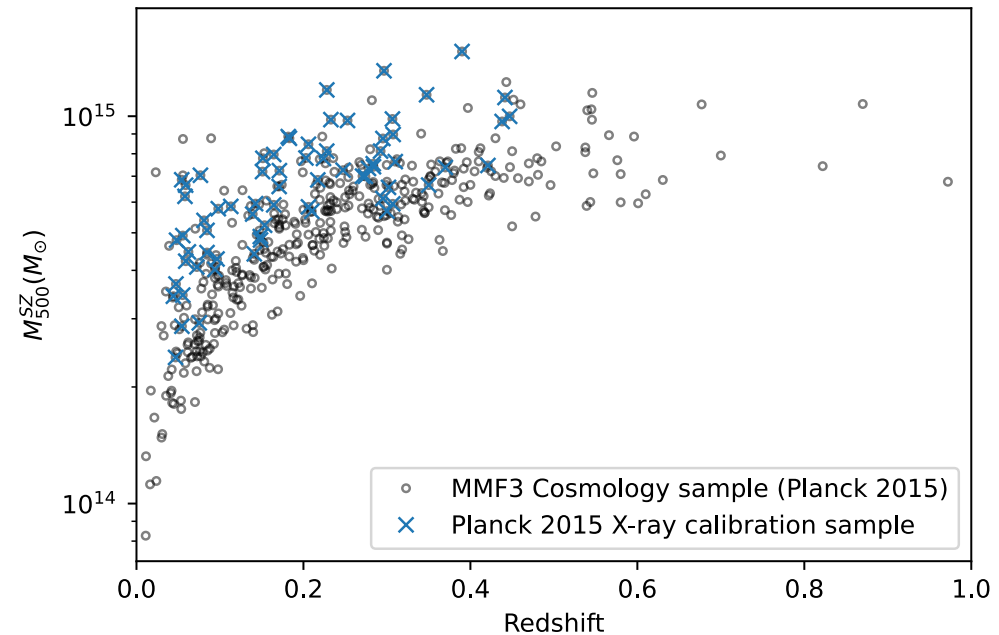
## Improving on Planck 2015: a better calibration sample

Planck data provides full sky SZ-survey: great opportunity for cosmological analysis

Cluster mass can't be directly inferred from SZ signal

Arnaud et al. 2010 relates X-ray signal from XMM-Newton to mass under hydrostatic equilibrium assumption

Y500-M500 is calibrated on a common XMM/SZ set of 71 clusters:  $E^{-2/3}(z) \left[ \frac{D_A^2 Y_{500}}{10^{-4} \text{ Mpc}^2} \right] = 10^{-0.19 \pm 0.02} \left( \frac{(1-b) M_{500}}{6 \times 10^{14} M_\odot} \right)^{1.79 \pm 0.08}$



# Combining X-ray and SZ

## Improving on Planck 2015: a better calibration sample

Planck data provides full sky SZ-survey: great opportunity for cosmological analysis

Cluster mass can't be directly inferred from SZ signal

Arnaud et al. 2010 relates X-ray signal from XMM-Newton to mass under hydrostatic equilibrium assumption

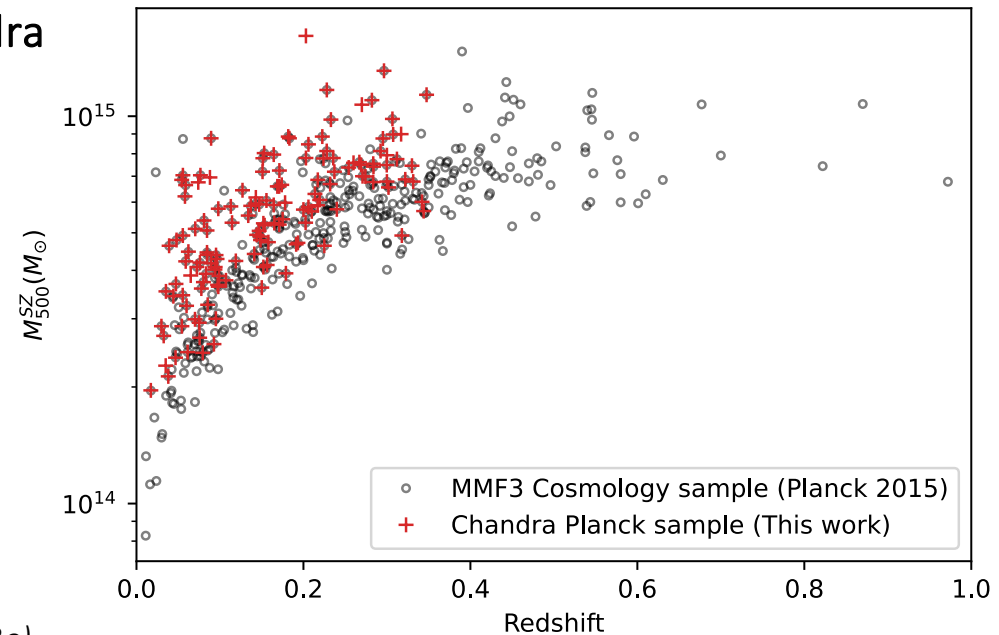
~~Y500 - M500 is calibrated on a common XMM/SZ set of 71 clusters:~~

$$E^{-2/3}(z) \left[ \frac{D_A^2 Y_{500}}{10^{-4} \text{ Mpc}^2} \right] = 10^{-0.19 \pm 0.02} \left( \frac{(1-b) M_{500}}{6 \times 10^{14} M_\odot} \right)^{1.79 \pm 0.08}$$

Full re-observation of Planck ESZ sample (with z<0.35) by Chandra



- SZ-selected sample
- More clusters (146 vs 71)
- Better low-mass leverage
- Similar high-mass leverage
- Better low-redshift leverage
- Slightly worse high-redshift leverage



# Combining X-ray and SZ

## Improving on Planck 2015: a better calibration sample

Planck data provides full sky SZ-survey: great opportunity for cosmological analysis

Cluster mass can't be directly inferred from SZ signal

Arnaud et al. 2010 relates X-ray signal from XMM-Newton to mass under hydrostatic equilibrium assumption

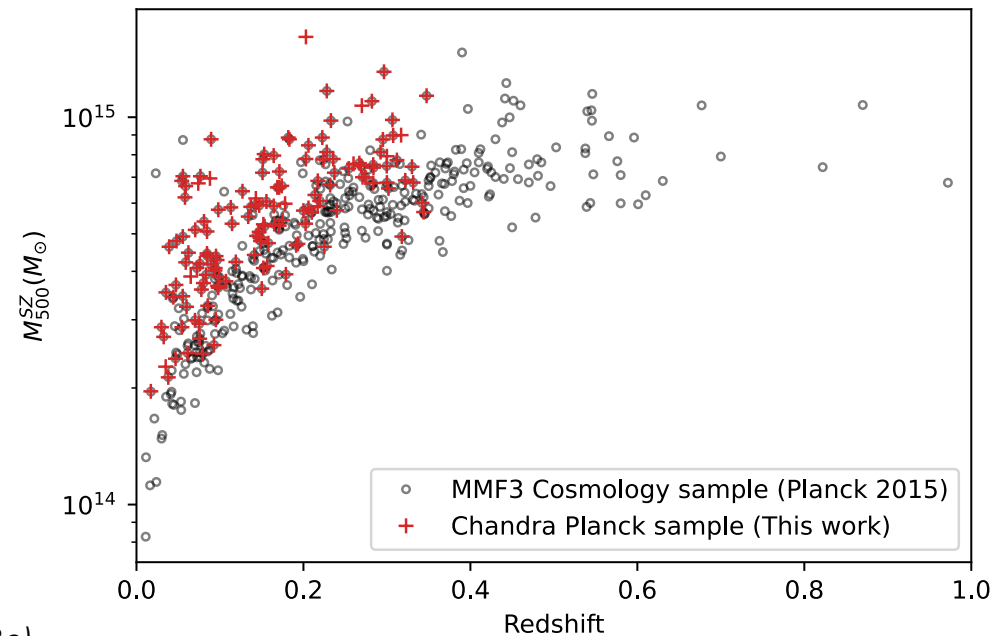
~~Y500 - M500 is calibrated on a common XMM/SZ set of 71 clusters:  $E^{-2/3}(z) \left[ \frac{D_A^2 Y_{500}}{10^{-4} \text{ Mpc}^2} \right] = 10^{-0.19+0.02} \left( \frac{(1-b) M_{500}}{6 \times 10^{14} M_\odot} \right)^{1.79 \pm 0.08}$~~

146 clusters from Planck ESZ sample were observed by

Chandra



Analyse the data and calibrate a new scaling relation  
Constrain cosmological parameters

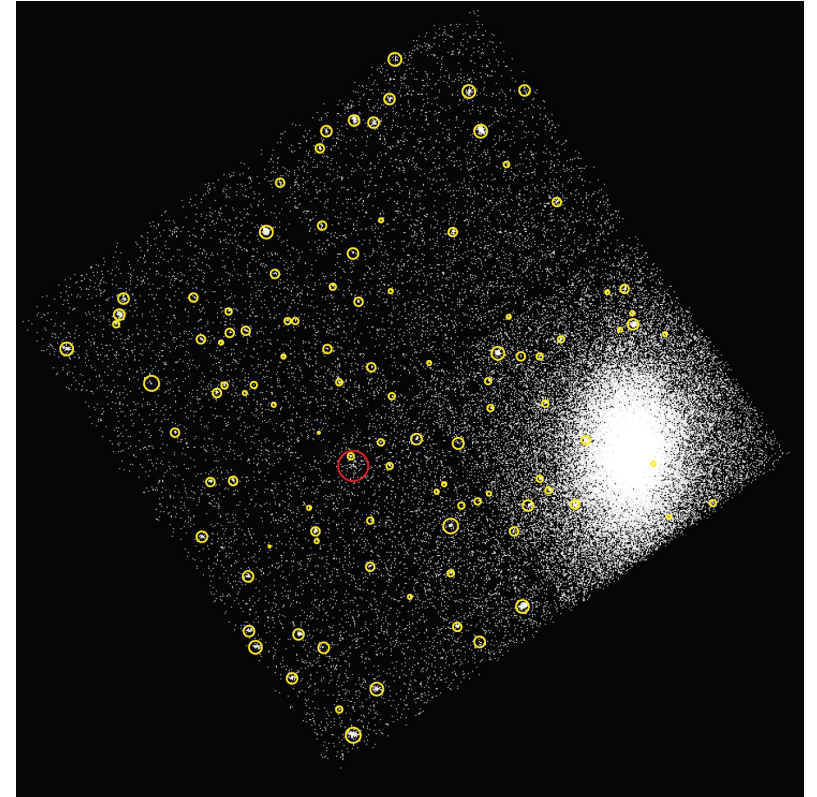




# Analysis of X-ray data

## Data processing: from event file to profiles

- Charge-transfer inefficiency, mirror contamination, CCD non-uniformity and time dependence of gain are corrected
- Blank sky and readout artifacts are subtracted
- X-ray point sources and extended substructures are masked
- Surface brightness profile is extracted in the 0.7-2keV band (better signal/noise ratio), in concentric annuli around emission peak
- Spectra are extracted in the 0.6-10keV band, and fitted with single temperature MEKAL model



Typical source subtraction, point sources are in yellow and extended source in red

# Analysis of X-ray data

## Calculating masses from X-ray: Yx scaling relation

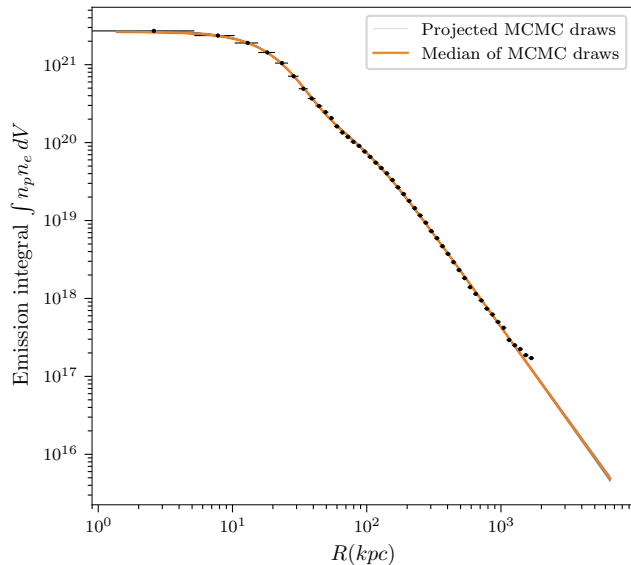
Use Vikhlinin et al. 2006 profile for density:

$$n_p n_e = n_0^2 \frac{(r/r_c)^{-\alpha}}{(1 + r^2/r_c^2)^{3\beta - \alpha/2}} \frac{1}{(1 + r^\gamma/r_s^\gamma)^{\epsilon/\gamma}} + \frac{n_{02}^2}{(1 + r^2/r_{c2}^2)^{3\beta_2}}$$

Project 3D profiles to compare to 2D observations

**Calculate masses** using Vikhlinin et al. 2009 Yx-M500 scaling relation:

Iterative process since Yx is measured within R500:



Fitted profile of Abell 2204

# Analysis of X-ray data

## Calculating masses from X-ray: Yx scaling relation

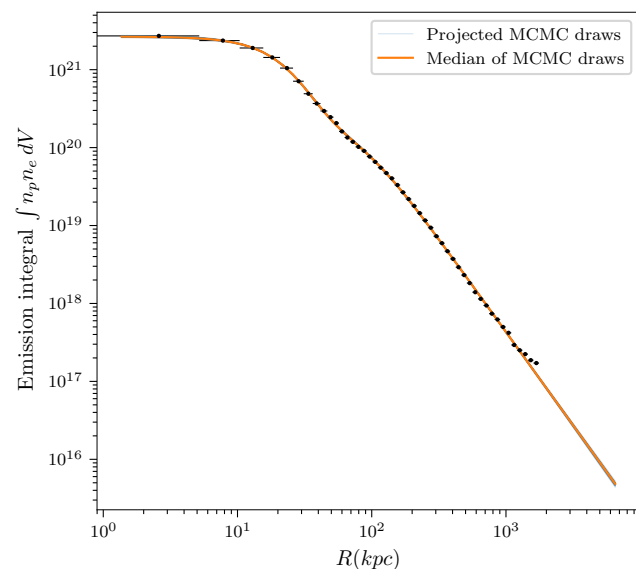
Use Vikhlinin et al. 2006 profile for density:

$$n_p n_e = n_0^2 \frac{(r/r_c)^{-\alpha}}{(1 + r^2/r_c^2)^{3\beta - \alpha/2}} \frac{1}{(1 + r^\gamma/r_s^\gamma)^{\epsilon/\gamma}} + \frac{n_{02}^2}{(1 + r^2/r_{c2}^2)^{3\beta_2}}$$

Project 3D profiles to compare to 2D observations

**Calculate masses** using Vikhlinin et al. 2009 Yx-M500 scaling relation:  
Iterative process since Yx is measured within R500:

1) First R500 value from T-M500 scaling relation (Vikhlinin et al. 2009)



Fitted profile of Abell 2204

# Analysis of X-ray data

## Calculating masses from X-ray: Yx scaling relation

Use Vikhlinin et al. 2006 profile for density:

$$n_p n_e = n_0^2 \frac{(r/r_c)^{-\alpha}}{(1 + r^2/r_c^2)^{3\beta - \alpha/2}} \frac{1}{(1 + r^\gamma/r_s^\gamma)^{\epsilon/\gamma}} + \frac{n_{02}^2}{(1 + r^2/r_{c2}^2)^{3\beta_2}}$$

Project 3D profiles to compare to 2D observations

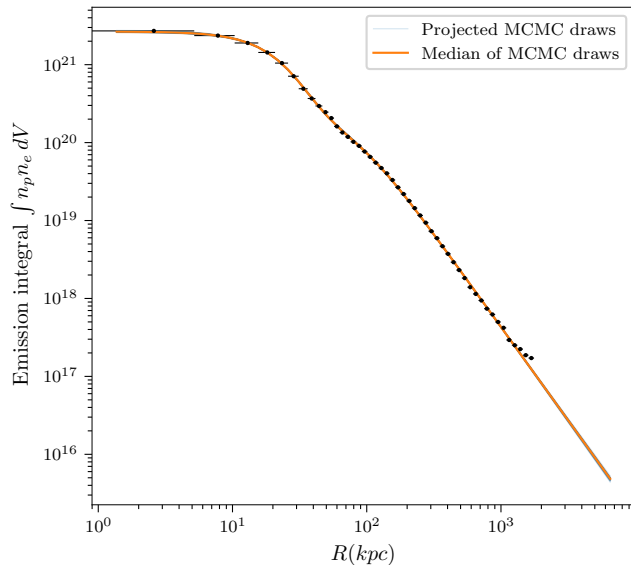
**Calculate masses** using Vikhlinin et al. 2009 Yx-M500 scaling relation:

Iterative process since Yx is measured within R500:

1) First R500 value from T-M500 scaling relation (Vikhlinin et al. 2009)

2) Measure core excised Tx in [0.15,1] R500,  $Y_X = k T_{exc} M_{gas}^{500}$

3) Solve  $\frac{4\pi}{3} 500 \rho_{crit}(z) R_{500}^3 = M_{500} = (5.77 \pm 0.20) \cdot 10^{14} h^{1/2} M_\odot \left( \frac{Y_X(R_{500})}{3 \cdot 10^{14} M_\odot \text{keV}} \right)^{0.57 \pm 0.03} E(z)^{-2/5}$   
for R500 (Vikhlinin et al. 2009)



Fitted profile of Abell 2204

# Analysis of X-ray data

## Calculating masses from X-ray: Yx scaling relation

Use Vikhlinin et al. 2006 profile for density:

$$n_p n_e = n_0^2 \frac{(r/r_c)^{-\alpha}}{(1 + r^2/r_c^2)^{3\beta - \alpha/2}} \frac{1}{(1 + r^\gamma/r_s^\gamma)^{\epsilon/\gamma}} + \frac{n_{02}^2}{(1 + r^2/r_{c2}^2)^{3\beta_2}}$$

Project 3D profiles to compare to 2D observations

**Calculate masses** using Vikhlinin et al. 2009 Yx-M500 scaling relation:

Iterative process since Yx is measured within R500:

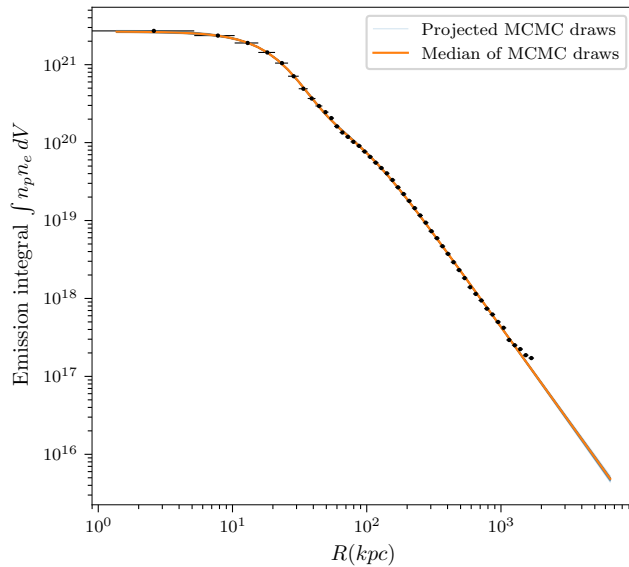
1) First R500 value from T-M500 scaling relation (Vikhlinin et al. 2009)

2) Measure core excised Tx in [0.15,1] R500,  $Y_X = k T_{exc} M_{gas}^{500}$

3) Solve  $\frac{4\pi}{3} 500 \rho_{crit}(z) R_{500}^3 = M_{500} = (5.77 \pm 0.20) \cdot 10^{14} h^{1/2} M_\odot \left( \frac{Y_X(R_{500})}{3 \cdot 10^{14} M_\odot \text{keV}} \right)^{0.57 \pm 0.03} E(z)^{-2/5}$   
for R500 (Vikhlinin et al. 2009)

4) Iterate 2)&3)

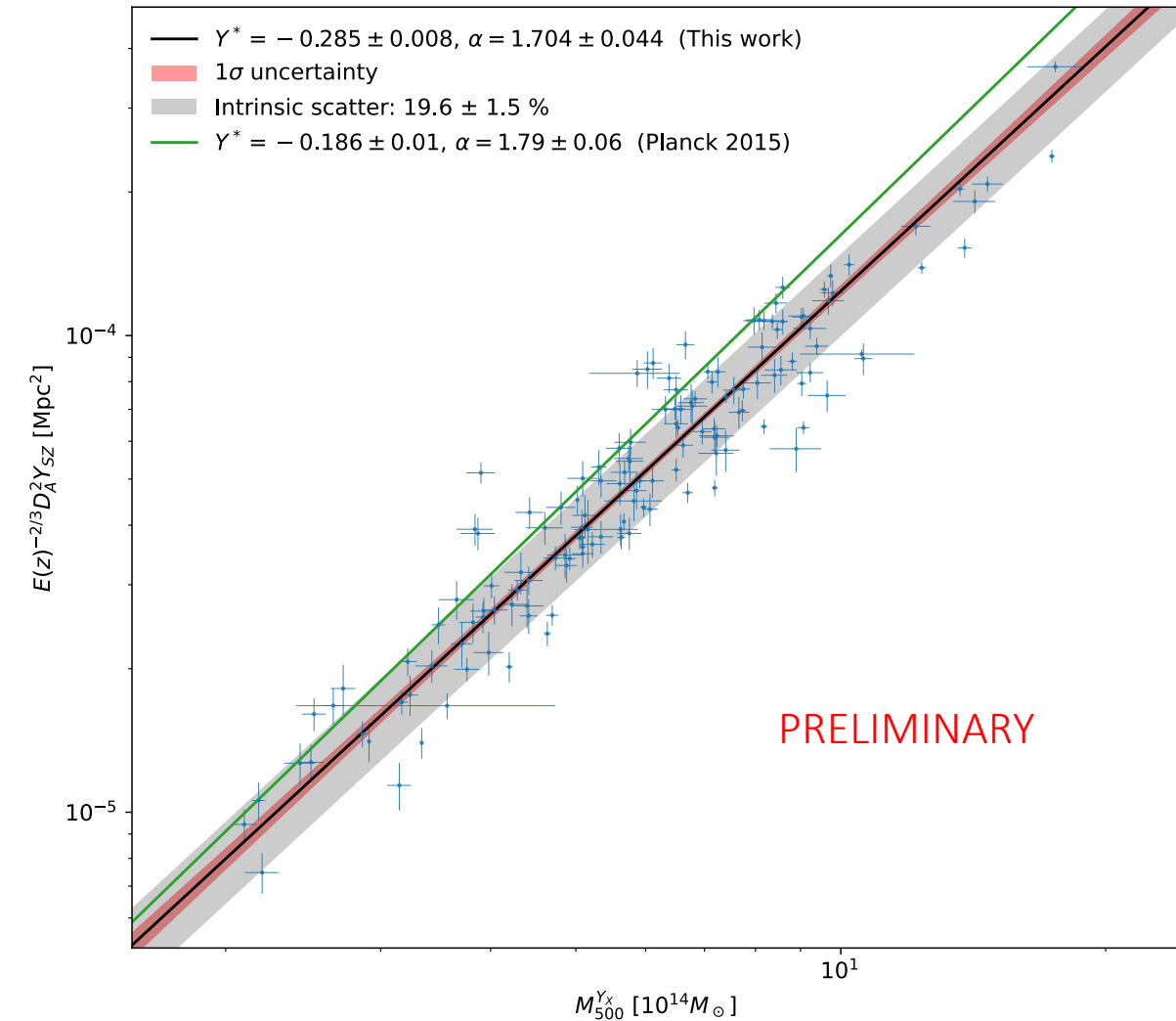
5)  $M_{500} = (5.77 \pm 0.20) \cdot 10^{14} h^{1/2} M_\odot \left( \frac{Y_X(R_{500})}{3 \cdot 10^{14} M_\odot \text{keV}} \right)^{0.57 \pm 0.03} E(z)^{-2/5}$



Fitted profile of Abell 2204

# Obtaining masses

## Calibrating the Ysz-M relation



Run MMF algorithm with X-ray positions and apertures  
Obtain Ysz with uncertainties

Correct for Malmquist bias:

Divide each individual Ysz by mean bias at that value

After adding statistical uncertainty and scatter from X-ray scaling relation:

$$E^{-2/3}(z) \frac{D_A^2 Y_{500}}{10^{-4} \text{Mpc}^2} = 10^{-0.29 \pm 0.01} \left( \frac{(1-b) M_{500}}{6 \cdot 10^{14} M_{\odot}} \right)^{1.70 \pm 0.1}$$

Scatter: 21%

Robust to linear regression method (emcee, LinMix, BCES)

# Obtaining masses

## Comparison with Planck 2015 results

Preliminary scaling relation:

$$E^{-2/3}(z) \frac{D_A^2 Y_{500}}{10^{-4} \text{Mpc}^2} = \underline{10^{-0.29 \pm 0.01}} \left( \frac{(1-b) M_{500}}{6 \cdot 10^{14} M_\odot} \right)^{\underline{1.70 \pm 0.1}} \quad \text{Scatter: 21\%}$$

Planck collab. 2015 Cosmology from SZ number counts scaling relation :

$$E^{-2/3}(z) \left[ \frac{D_A^2 Y_{500}}{10^{-4} \text{Mpc}^2} \right] = \underline{10^{-0.19 \pm 0.02}} \left( \frac{(1-b) M_{500}}{6 \times 10^{14} M_\odot} \right)^{\underline{1.79 \pm 0.08}} \quad \text{Scatter: 18\%}$$

The new scaling relation has:

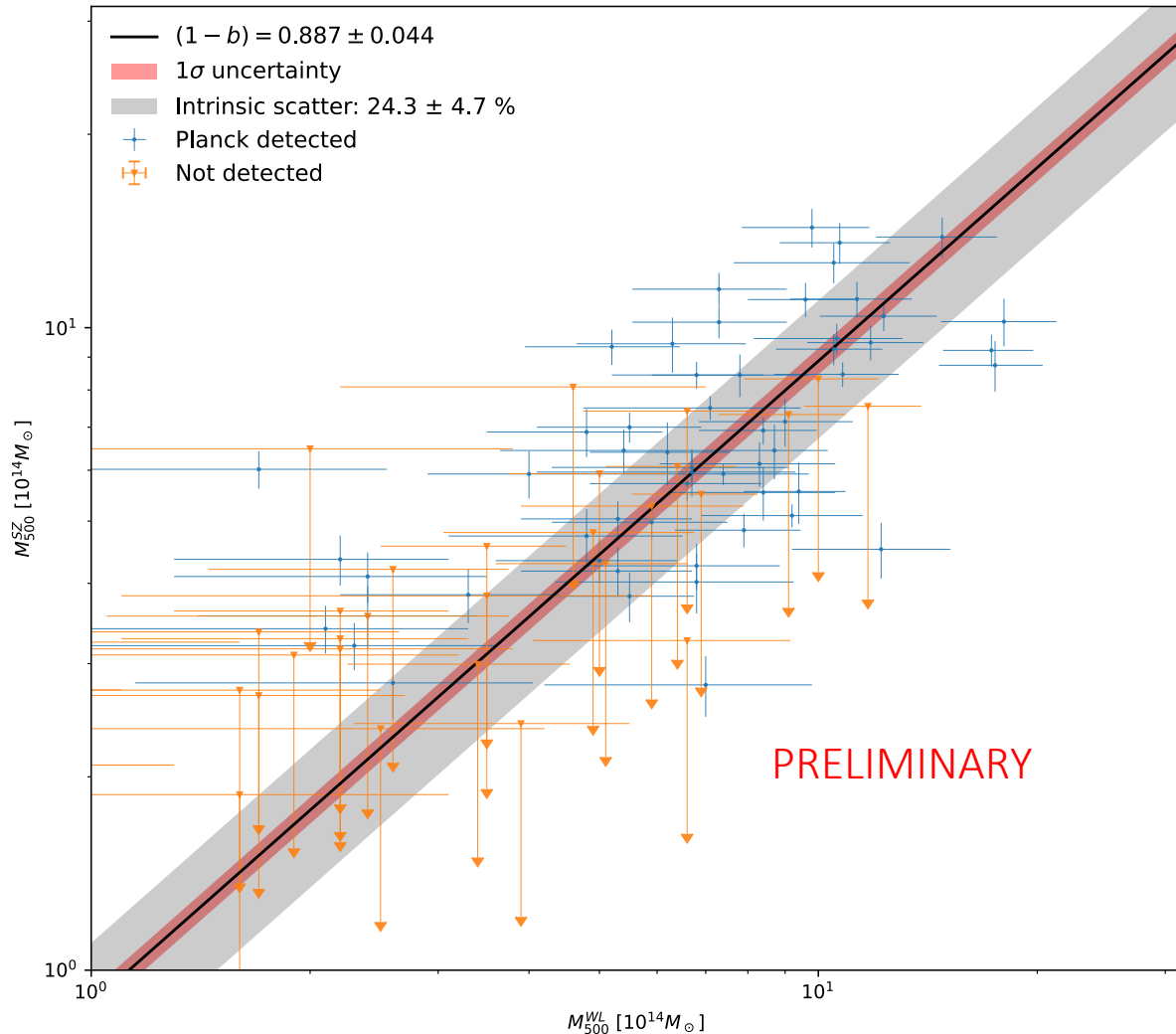
**Lower normalization:** Chandra and XMM temperature calibration don't match, Chandra measures hotter and thus heavier cluster. The **difference is coherent with predictions from Schellenberger et al. 2015** (20% difference)

**Shallower slope:** The new scaling relation is closer to self-similar (slope of 5/3)

**Comparable uncertainties:** Lower uncertainties on  $Y_{\text{SZ}}-M_{Y_X}$  (larger sample) but higher uncertainties on  $Y_X-M_{Y_X}$  compensates the difference

# Obtaining masses

## Calibrating the hydrostatic mass bias



X-Ray masses are obtained under the assumption of hydrostatic equilibrium (i.e. thermal pressure perfectly balancing gravity)

Non thermal pressure support and deviations from equilibrium lead to **under-estimation of the true mass**

Effect accounted for by a **multiplicative factor, calibrated with weak lensing mass estimates**

$$E^{-2/3}(z) \frac{D_A^2 Y_{500}}{10^{-4} \text{Mpc}^2} = 10^{-0.29 \pm 0.01} \left( \frac{(1 - b) M_{500}}{6 \cdot 10^{14} M_\odot} \right)^{1.70 \pm 0.1}$$

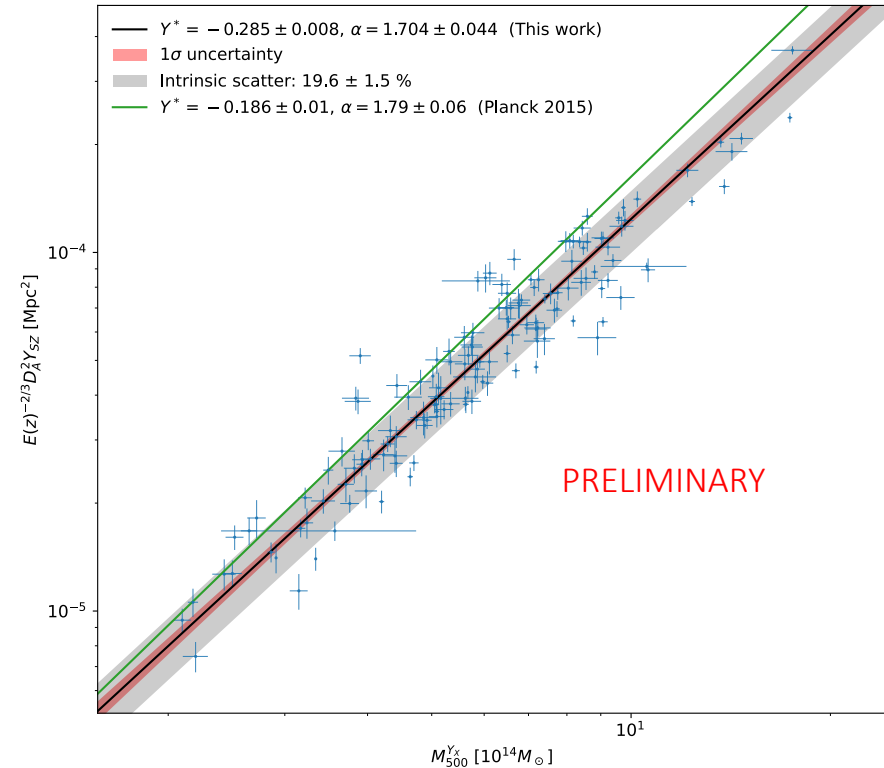
Use WL data from Herbonnet et al. 2020

Calibration sample	D+nD	D
Chandra	$0.89 \pm 0.04$	$0.91 \pm 0.05$
XMM-Newton	$0.76 \pm 0.04$	$0.78 \pm 0.04$
Herbonnet+20	X	$0.81 \pm 0.04$
CCCP (P15)	X	$0.78 \pm 0.09$



# Constraining the cosmology

What are the effect of changing the scaling relation ?



Rest of the analysis is identical to Planck 2015 Cosmology with SZ number counts:

Use **cosmology cluster sample**, **two dimensional likelihood** (fit number counts as function of redshift and S/N), **additional priors from BBN and BAO** (only  $\Omega_m$  and  $\sigma_8$  are constrained by cluster number counts)

$$\frac{dN}{dzdq} = \int d\Omega_{\text{mask}} \int dM_{500} \frac{dN}{dzdM_{500}d\Omega} P[q|\bar{q}_m(M_{500}, z, l, b)] \quad \text{Fitted number counts}$$

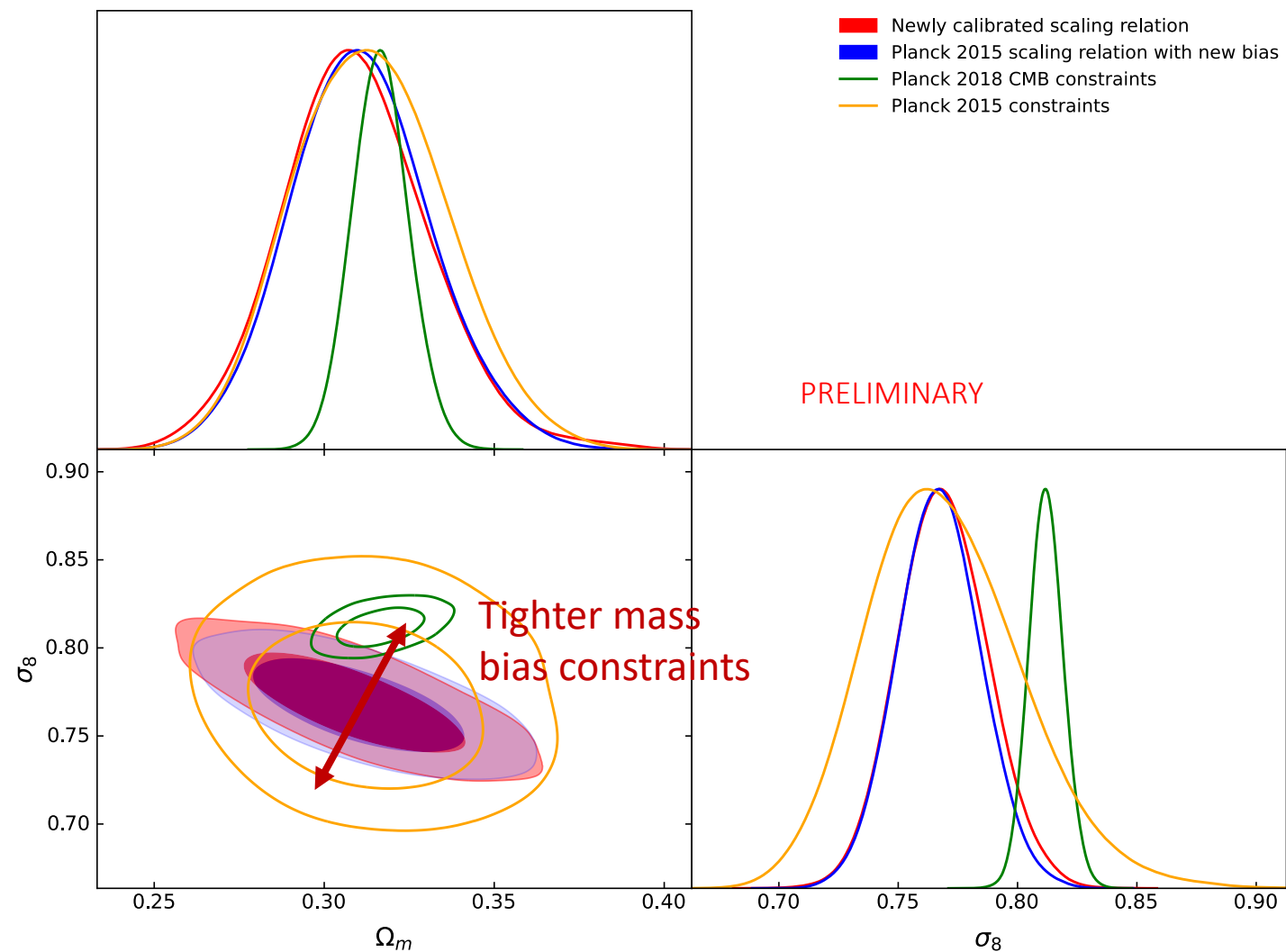
$$\frac{dN}{dzdM_{500}d\Omega} = \frac{dN}{dVdM_{500}} \frac{dV}{dzd\Omega} \quad \text{Theoretical mass function}$$

$$\bar{q}_m \equiv \bar{Y}_{500}(M_{500}, z) / \sigma_f[\bar{\theta}_{500}(M_{500}, z), l, b] \quad \text{Median S/N for given M and z}$$

Scaling relation

# Constraining the cosmology

What are the effect of changing the scaling relation ?



Cosmological constraints obtained:

X-ray sample	$\Omega_m$	$\sigma_8$
Chandra	$0.308 \pm 0.022$	$0.764 \pm 0.019$
XMM-Newton	$0.311 \pm 0.020$	$0.755 \pm 0.019$

Even with calibration problems between the two telescopes, the constraints are fully consistent

Constraints are centered on the same value and tighter than Planck 2015, thus in higher tension with the CMB

Mass calibration, and mass bias in particular is the most sensitive point of cluster cosmology

# Constraining the cosmology

Next step: internal calibration

$$E^{-2/3}(z) \frac{D_A^2 Y_{500}}{10^{-4} \text{Mpc}^2} = 10^{-0.29 \pm 0.01} \left( \frac{(1-b)M_{500}}{6 \cdot 10^{14} M_\odot} \right)^{1.71 \pm 0.1}$$



$$E^{-\beta}(z) \frac{D_A^2 Y_{500}}{10^{-4} \text{Mpc}^2} = Y_* \left( \frac{h}{0.7} \right)^{-2+\alpha} \left( \frac{(1-b)M_{500}}{6 \cdot 10^{14} M_\odot} \right)^\alpha$$

Include X-ray, SZ (and lensing data ?) in the likelihood and fit cosmological parameters and  $\alpha$ ,  $\beta$ ,  $Y_*$  and  $b$  together



Obtain cosmological constraints from clusters using multi-wavelength information and marginalising over systematics

Other possible improvements: Use PR4 maps for SZ detections, explore other (lower uncertainty) mass estimates...

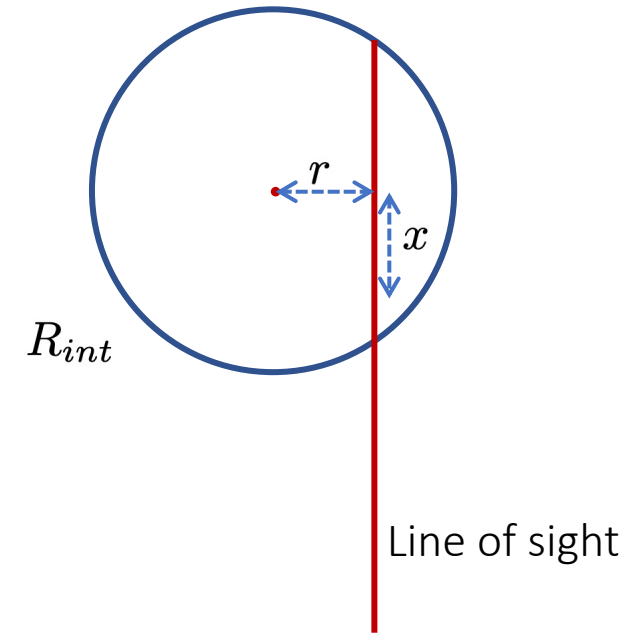
# Appendix

## Dealing with projection effects

The functions are made to fit 3D profiles, but observations are 2D projections along the line of sight  
During fitting, 3D profiles are first projected then compared to 2D observations

In the case of density/emission integral we can neglect the bin width:

$$EI_i = 2 \int_0^{\sqrt{R_{int}^2 - r_i^2}} n_p n_e (\sqrt{x^2 + r_i^2}) dx \quad \text{where } R_{int} = 50R_{500}$$



In the case of temperature, we need to weight by density, account for a dependence on temperature (Mazzotta et al. 2004), and take bin width into account:

$$T_i = \frac{\int_{r_i}^{r_{i+1}} \int_1^{\sqrt{(R_{int})^2 - r^2}} r w T_{\text{fit}}(\sqrt{r^2 + x^2}) dx dr}{\int_{r_i}^{r_{i+1}} \int_1^{\sqrt{(R_{int})^2 - r^2}} r w dx dr} \quad \text{where } w = n_p n_e (\sqrt{r^2 + x^2}) T_{\text{fit}}^{-0.75}(\sqrt{r^2 + x^2}) \text{ and } R_{int} = R_{200}$$

# Appendix

## Masses from X-ray data

With X-ray data, we can compute masses under hydrostatic equilibrium assumption:

$$M_{HE}(< r) = -\frac{rk_B T(r)}{G\mu m_p} \left( \frac{d \ln \rho(r)}{d \ln r} + \frac{d \ln T(r)}{d \ln r} \right)$$

But clusters' dynamical states vary widely and the assumption can be quite false

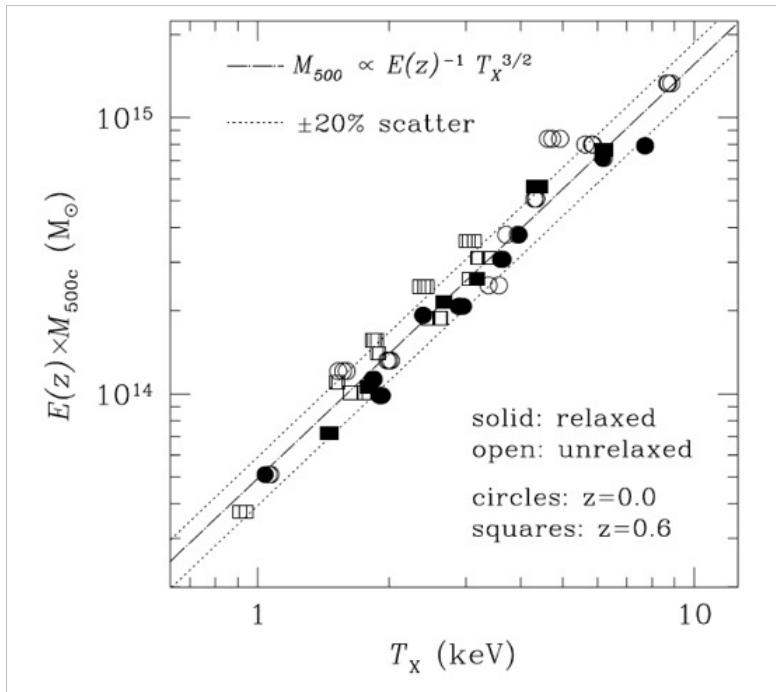
Instead of using the hydrostatic masses, scaling relations are commonly used:

- Calibrate relation between observable/hydrostatic mass for a set of relaxed clusters
- Use the relation to calculate other cluster masses

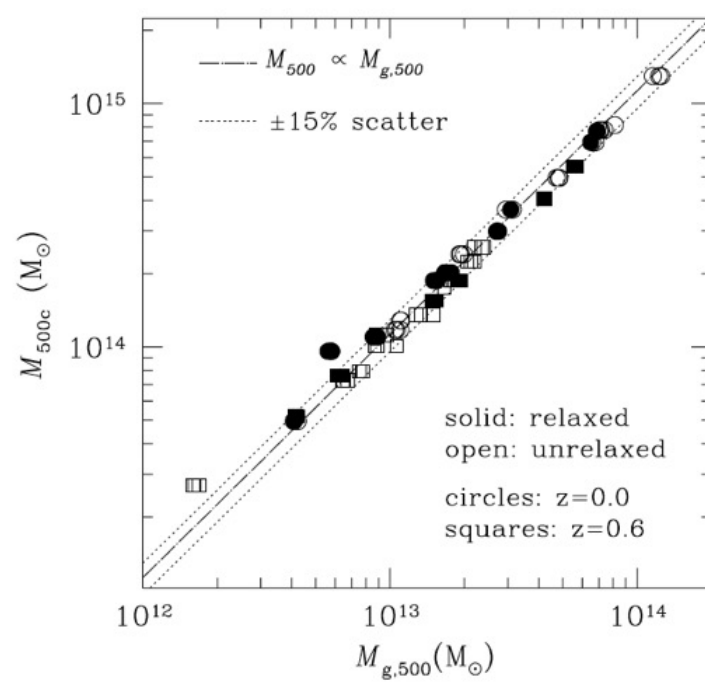
# Appendix

## What is the best proxy for mass ?

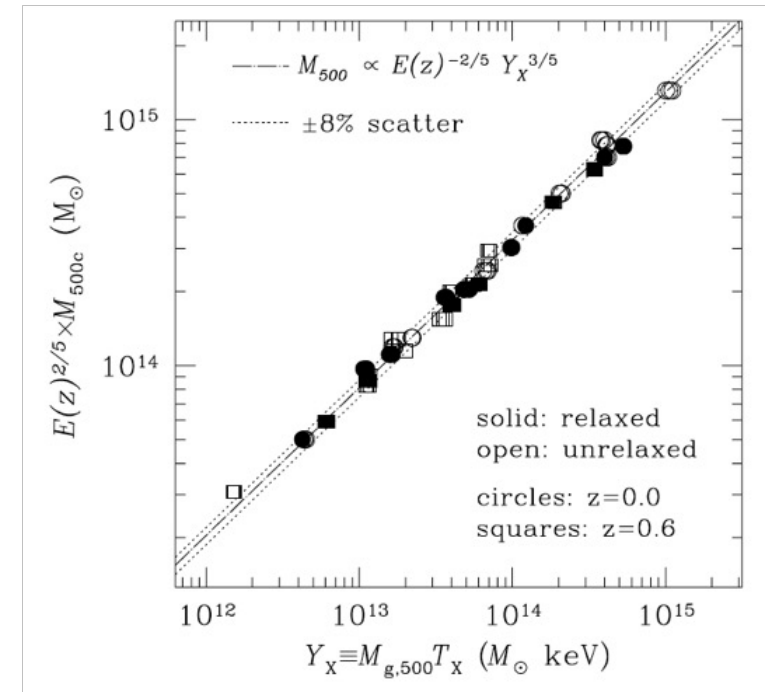
Kravtsov et al. 2006: comparison of proxies/true mass on simulated Chandra observations of clusters



20% scatter due to unrelaxed clusters mostly  
 Unrelaxed cluster have lower  $T_x$ :  
 Kinetic energy not fully converted to thermal during mergers  
 Slope=self similarity



15% scatter  
 Slope!=self similarity ( $0.92 \pm 0.02$ )  
 Due to  $f_{\text{gas}}$  varying with  $M$  &  $z$



8% scatter  
 No relaxed/unrelaxed distinction  
 Less sensitive to departure from spherical symmetry  
 Slope=self similarity

$Y_x$  is a robust and self-similar proxy to mass

# Appendix

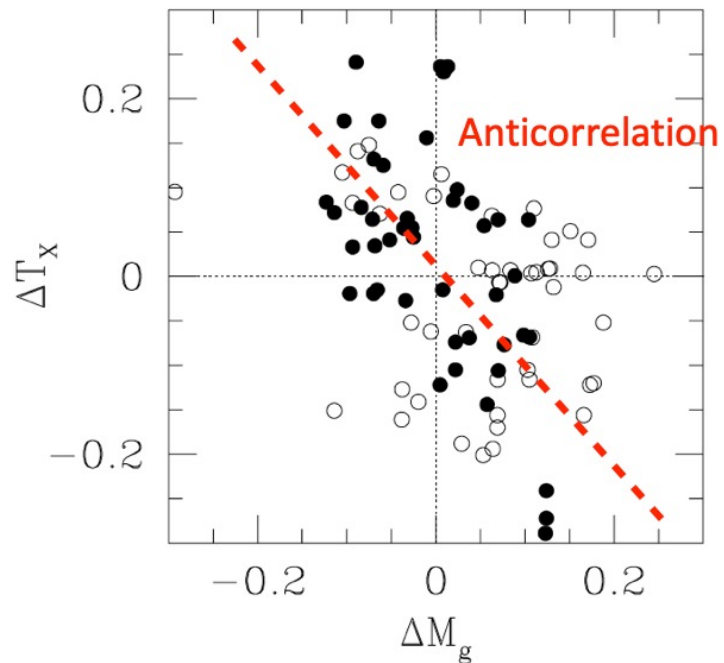


FIG. 5.—Fractional deviations in temperature and gas mass for fixed  $M_{500}$  relative to their respective best-fit self-similar relations,  $M_{500} \propto T_x^{1.5}$  and  $M_{500} \propto M_{g,500}$ . The fit includes all systems, at both  $z = 0$  (filled circles) and  $z = 0.6$  (open circles). Note that the deviations for gas mass and temperature are generally anticorrelated: clusters with large positive (negative) deviations in  $M_{g,500}$  tend to have negative (positive) deviations in  $T_x$ . A similar anticorrelation exists in the trend with redshift (compare the distribution of points for  $z = 0$  and  $0.6$ ). [See the electronic edition of the Journal for a color version of this figure.]

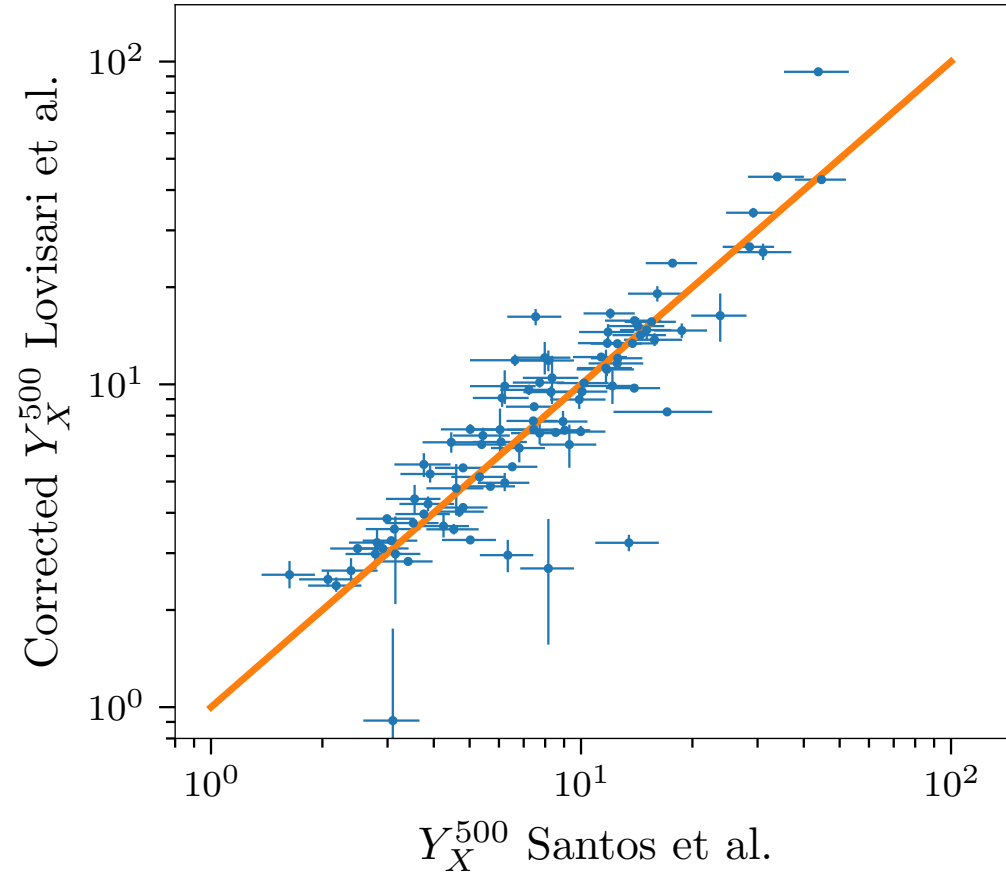
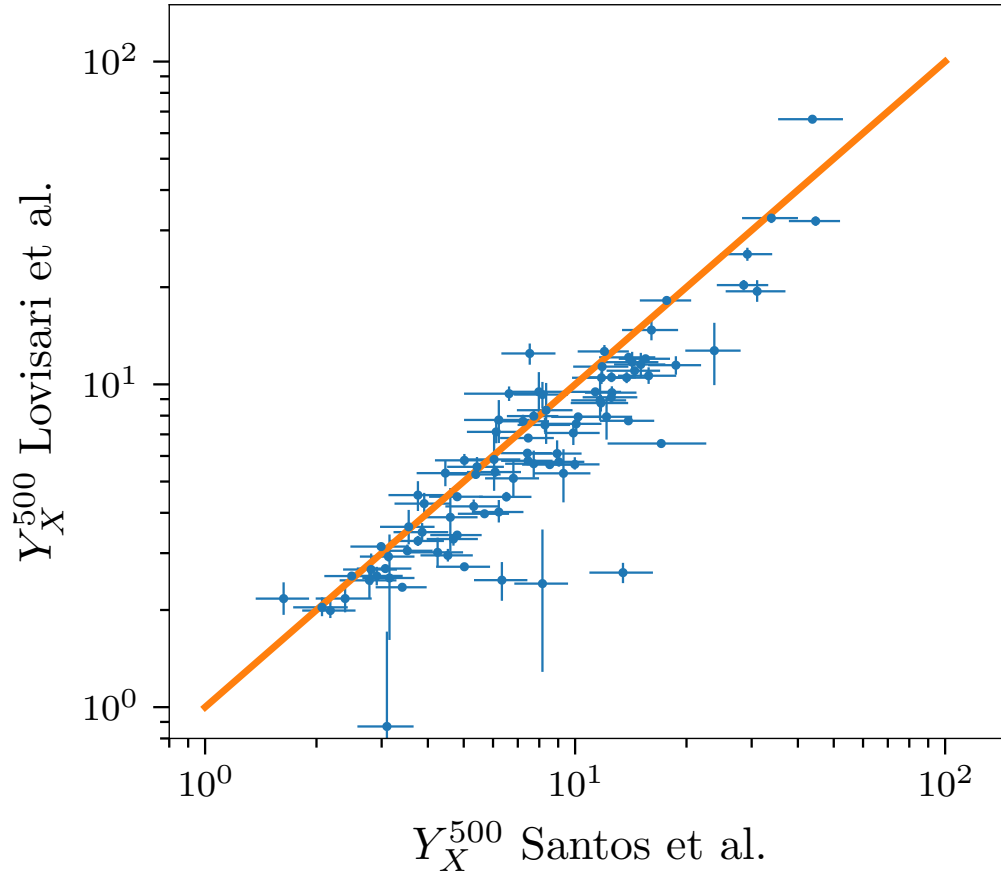
Why is  $Y_x$  a good proxy ?

Less relaxed clusters, over-estimation of  $M_g$  (non-uniform density,  $\langle n^2 \rangle > \langle n \rangle^2$ )  
Unrelaxed cluster have lower  $T_x$ : kinetic energy not fully converted to thermal during mergers

# Appendix

## XMM Newton vs Chandra

Temperature measurements don't match, leading to different  $Y_x$  values



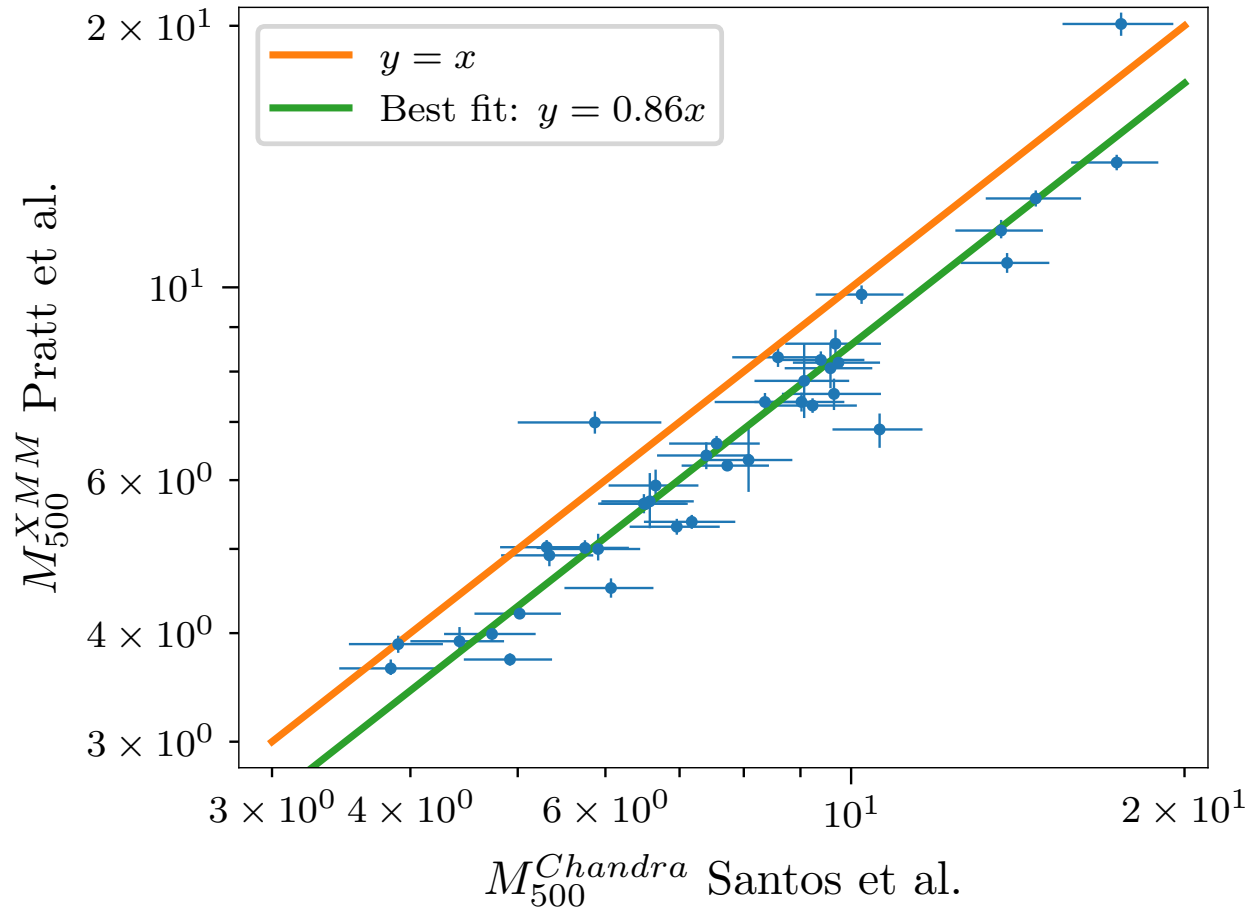
The temperature calibration can be accounted for, but the truth isn't known



# Appendix

## XMM Newton vs Chandra

Because the true temperature isn't known, and  $Y_x$ - $M_{500}$  relations rely on HSE hypothesis, the masses inferred from Chandra and XMM differ



XMM scaling relation (Arnaud et al. 2010):

$$h(z)^{2/5} M_{500} = 10^{14.567 \pm 0.010} \left[ \frac{Y_X}{2 \times 10^{14} h_{70}^{-5/2} M_{\odot} \text{ keV}} \right]^{0.561 \pm 0.018} h_{70}^{-1} M_{\odot}$$

Chandra scaling relation (Vikhlinin et al. 2009):

$$M_{500}^{Y_X} = E^{-2/5}(z) A_{YM} \left[ \frac{Y_X}{3 \times 10^{14} M_{\odot} \text{ keV}} \right]^{B_{YM}}$$

$$A_{YM} = (5.77 \pm 0.20) \times 10^{14} h^{1/2} M_{\odot}$$

$$B_{YM} = 0.57 \pm 0.03$$

Schellenberger et al. 2015:

$$M_{500}^{XMM} = 0.859_{0.016}^{+0.017} \cdot M_{500}^{Chandra})^{1.00 \pm 0.02}$$

The masses obtained from  $Y_x$  with XMM are 14% lower on average

# Appendix

## Malmquist bias

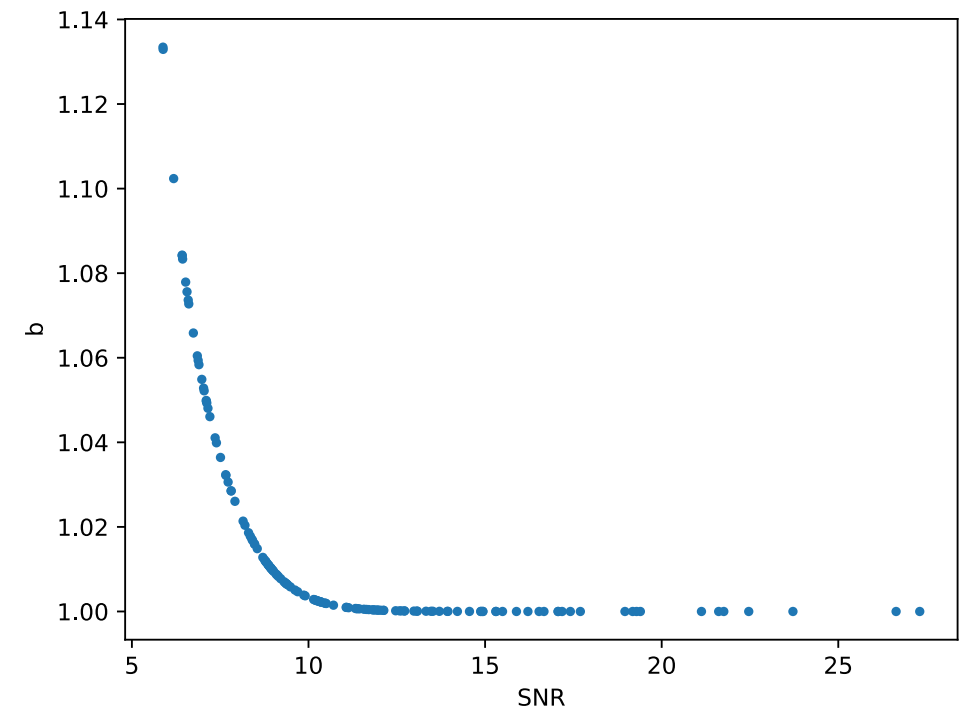
When studying the relation between signal and another observable for a signal-to-noise limited sample, the intrinsic scatter in the relation will lead to preferential detection of objects biased high w.r.t. the mean in the low signal range

This needs to be accounted for when calibrating a scaling relation, by dividing each  $Y_{SZ}$  by the mean bias at the corresponding signal to noise ratio

$$Y_{SZ}^{corrected} = Y_{SZ}/b$$

$$\ln b = \frac{\exp(-x^2/2\sigma^2)}{\sqrt{\pi/2} \operatorname{erfc}(-x/\sqrt{2}\sigma)} \sigma$$

$$\text{where } x = -\log\left(\frac{(S/N)}{(S/N)_{cut}}\right) \text{ and } \sigma = \sqrt{\ln[((S/N) + 1)/(S/N)]^2 + (\ln 10 \sigma_{int})^2}$$



# Appendix

What are the effect of changing the scaling relation ?

Lower normalisation: heavier clusters, higher  $S_8$

Change of slope: modifies ratio of high to low mass clusters, moves constraints along  $\sigma_8$ - $\Omega_m$  degeneracy

